

13. Maguire, W. C., Hanel, R. A., Jennings, D. E., Kunde, V. G. & Samuelson, R. E. C_3H_8 and C_3H_4 in Titan's atmosphere. *Nature* **292**, 683–686 (1981).
14. Kunde, V. G. *et al.* C_4H_2 , HC_3N , and C_2N_2 in Titan's atmosphere. *Nature* **292**, 686–688 (1981).
15. Khare, B. N. *et al.* Optical constants of organic tholins produced in a simulated Titanian atmosphere: from soft X-ray to microwave frequencies. *Icarus* **60**, 127–137 (1984).
16. McKay, C. P., Pollack, J. B. & Courtin, R. The thermal structure of Titan's atmosphere. *Icarus* **80**, 23–53 (1989).
17. Danielson, R. E., Caldwell, J. J. & Larach, D. R. An inversion in the atmosphere of Titan. *Icarus* **20**, 437–443 (1973).
18. McKay, C. P., Pollack, J. B. & Courtin, R. The greenhouse and antighreenhouse effects on Titan. *Science* **253**, 1118–1123 (1991).
19. Hutzell, W. T., McKay, C. P. & Toon, O. B. Effects of the time-varying haze production on Titan's geometric albedo. *Icarus* **105**, 162–174 (1993).
20. Pollack, J. B., Rages, K., Toon, O. B. & Yung, Y. L. On the relationship between secular brightness changes of Titan and solar variability. *Geophys. Res. Lett.* **7**, 829–832 (1980).
21. Allen, M., Pinto, J. P. & Yung, Y. L. Titan: aerosol photochemistry and variations related to sunspot cycle. *Astrophys. J.* **242**, L125–L128 (1980).
22. Rannou, P., Cabane, M. & Chassefière, E. Growth of aerosols in Titan's atmosphere and related time scales: A stochastic approach. *Geophys. Res. Lett.* **20**, 967–970 (1993).
23. Toon, O. B., McKay, C. P., Griffith, C. A. & Turco, R. P. A physical model of Titan aerosols. *Icarus* **95**, 24–53 (1992).
24. Hutzell, W. T., McKay, C. P., Toon, O. B. & Houdin, F. Simulations of Titan's brightness by a two dimensional haze model. *Icarus* **119**, 112–129 (1995).
25. Cabane, M., Chassefière, E. & Israel, G. Formation and growth of photochemical aerosols in Titan's atmosphere. *Icarus* **96**, 176–189 (1992).
26. Cabane, M., Rannou, P., Chassefière, E. & Israel, G. Fractal aggregates in Titan's atmosphere. *Planet. Space Sci.* **41**, 257–267 (1993).
27. Lebonnois, S., Toubanc, D., Houdin, F. & Rannou, P. Seasonal variations of Titan's atmospheric composition. *Icarus* **152**, 384–406 (2001).
28. Rannou, P., McKay, C. P., Botet, R. & Cabane, M. Semi-empirical model of absorption and scattering by isotropic fractal aggregates of spheres. *Planet. Space Sci.* **47**, 385–396 (1999).

Acknowledgements

This work was partially supported by the NASA Planetary Atmospheres Program and the French Programme National de Planétologie. P.R. thanks the National Research Council Associateship Program.

Competing interests statement

The authors declare that they have no competing financial interests.

Correspondence and requests for materials should be addressed to P.R. (e-mail: pra@ccr.jussieu.fr).

Emergent excitations in a geometrically frustrated magnet

S.-H. Lee*, C. Broholm†, W. Ratcliff‡, G. Gasparovic†, Q. Huang*
T. H. Kim‡§ & S.-W. Cheong‡

* NIST Center for Neutron Research, National Institute of Standards and Technology, Gaithersburg, Maryland 20899, USA

† Department of Physics and Astronomy, The Johns Hopkins University, Baltimore, Maryland 21218, USA

‡ Department of Physics and Astronomy, Rutgers University, Piscataway, New Jersey 08854, USA

Frustrated systems are ubiquitous^{1–3}, and they are interesting because their behaviour is difficult to predict; frustration can lead to macroscopic degeneracies and qualitatively new states of matter. Magnetic systems offer good examples in the form of spin lattices, where all interactions between spins cannot be simultaneously satisfied⁴. Here we report how unusual composite spin degrees of freedom can emerge from frustrated magnetic interactions in the cubic spinel $ZnCr_2O_4$. Upon cooling, groups of six spins self-organize into weakly interacting antiferromagnetic loops, whose directors—the unique direction along which the spins are aligned, parallel or antiparallel—govern all low-tem-

perature dynamics. The experimental evidence comes from a measurement of the magnetic form factor by inelastic neutron scattering; the data show that neutrons scatter from hexagonal spin clusters rather than individual spins. The hexagon directors are, to a first approximation, decoupled from each other, and hence their reorientations embody the long-sought local zero energy modes for the pyrochlore lattice.

Magnetism in transition metal oxides stems from atomic spins on the vertices of a periodic lattice. In insulators, interactions generally favour antiparallel nearest-neighbour spin alignment. For a simple cubic lattice (Fig. 1a), only a long-range ordered spin configuration can satisfy all interactions. On cooling, such systems show a continuous increase in the spin correlation length, culminating in a phase transition to long-range order. But for spins on the vertices of corner-sharing tetrahedra (Fig. 1b), no configuration can satisfy all interactions—a magnetic predicament called ‘geometrical frustration’⁴. Because the spin interaction energy is minimized when the four spins on each tetrahedron add to zero, interactions do not call for a divergent correlation length, but simply define a restricted phase space for fluctuations, parametrized by θ and ϕ (Fig. 1b) for each tetrahedron^{5,6}. Just as composite fermions can emerge from degenerate Landau levels in a two-dimensional electron gas⁷, the near-degenerate manifold of states in a frustrated magnet is fertile ground for emergent behaviour⁸.

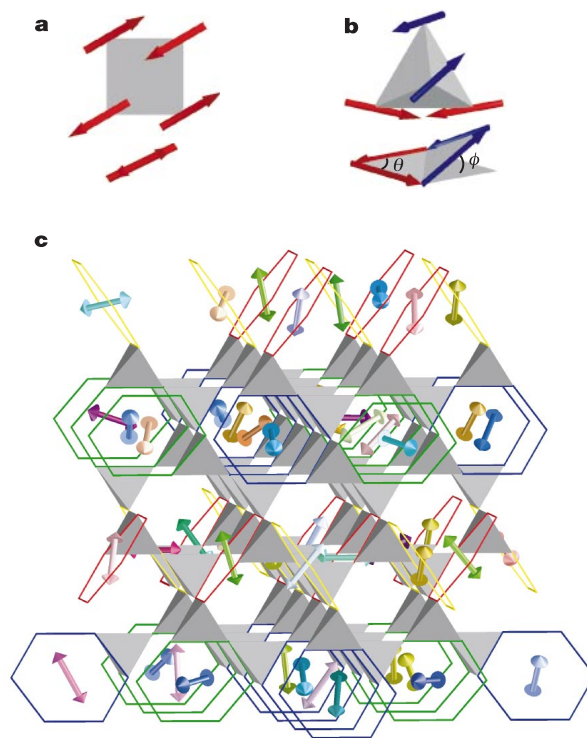


Figure 1 Lowest-energy spin configurations for four antiferromagnetically interacting spins on a square, a tetrahedron, and the pyrochlore lattice of corner-sharing tetrahedra. **a**, Setting aside global rotations, four spins on the vertices of a square with nearest-neighbour interactions have a unique lowest-energy spin configuration. **b**, For four spins on the vertices of a tetrahedron, any configuration with vanishing total spin has the lowest configuration energy. **c**, The lattice of corner-sharing tetrahedra formed by the octahedrally coordinated B sites in a spinel structure with chemical formula AB_2O_4 . A periodic assignment of all spins in the pyrochlore lattice is made to four different types of non-overlapping hexagons, represented by the colours blue, green, red and gold. Every spin belongs to just one hexagon, and each such hexagon carries a six spin director. The resulting tetragonal structure of these hexagons has a unit cell of $2a \times 2a \times 3c$, and can be described by a stacking of two different types of three-layer slabs along the c axis. The hexagon coverage on consecutive slabs is in fact uncorrelated, so that a macroscopic number of random slab-sequences can be generated.

§ Present address: Francis Bitter Magnet Laboratory, Massachusetts Institute of Technology, Cambridge, Massachusetts 02139, USA.

Although direct structural probes are unavailable for quantum Hall samples, we can monitor the correlated spin state in a frustrated magnet by scattering neutrons from it⁹. Neutrons carry a magnetic dipole moment, and are subject to forces from atomic-scale field gradients. The resulting pattern of quasi-elastic scattering versus wavevector transfer, $\mathbf{Q} = \mathbf{k}_i - \mathbf{k}_f$, is the sample-averaged Fourier transform of spin configurations within a coherence volume of order $(100 \text{ \AA})^3$ given by the instrumental resolution. Here \mathbf{k}_i and \mathbf{k}_f are the de Broglie wavevectors associated with the incident and scattered neutrons, respectively. Magnetic peaks generally sharpen with decreasing temperature as the correlation length, ξ , increases. For un-frustrated La_2CuO_4 (ref. 10), the half-width at half-maximum (HWHM), $\kappa(T) = \xi(T)^{-1}$, becomes indistinguishable from zero below a microscopic energy scale, the Curie–Weiss temperature $|\Theta_{\text{CW}}|$. In contrast, for frustrated ZnCr_2O_4 (Fig. 2), κ remains finite even below $|\Theta_{\text{CW}}|$, and extrapolates to a finite value as $T/|\Theta_{\text{CW}}| \rightarrow 0$.

The finite low-temperature correlation length in ZnCr_2O_4 signals the emergence of confined nanometre-scale spin clusters. Rather than being associated with temperature-dependent short-range order above a phase transition, the wavevector dependence of the low-temperature intensity (Fig. 3a, b) can be interpreted as a spin cluster form factor. As opposed to the form factor for an atomic spin, the cluster form factor vanishes for $Q \rightarrow 0$, which is evidence that clusters carry no net spin¹¹. Further analysis is complicated by the anisotropy of spin clusters, which can occur in four different orientations for a cubic crystal. Rather than Fourier-inverting the data, we therefore compare them to the orientationally averaged Fourier transform of potential spin clusters. Individual tetrahedra would be prime candidates, as they constitute the basic motif of the pyrochlore lattice. However, a tetrahedron is too small to account for the features observed (Fig. 3a, b). The next-smallest symmetric structural unit is the hexagonal loop formed by a cluster of six tetrahedra (Fig. 4a). Two spins from each tetrahedron occupy the vertices of a hexagon, while the other two spins from each tetrahedron belong to different hexagons. Averaging over the four different hexagon orientations in the pyrochlore lattice, the square of the antiferromagnetic hexagon spin-loop form factor can be

written as

$$|F_6(\mathbf{Q})|^2 \propto \left\{ \sin \frac{\pi}{2} h \cdot \left(\cos \frac{\pi}{2} k - \cos \frac{\pi}{2} l \right) \right\}^2 + \left\{ \sin \frac{\pi}{2} k \cdot \left(\cos \frac{\pi}{2} l - \cos \frac{\pi}{2} h \right) \right\}^2 + \left\{ \sin \frac{\pi}{2} l \cdot \left(\cos \frac{\pi}{2} h - \cos \frac{\pi}{2} k \right) \right\}^2$$

The magnetic neutron scattering intensity would follow $I_0(\mathbf{Q}) = |F_6(\mathbf{Q})|^2 |F(\mathbf{Q})|^2$, where $F(\mathbf{Q})$ is the magnetic form factor for Cr^{3+} . The excellent qualitative agreement between model and data in Fig. 3 provides compelling evidence that neutrons scatter from antiferromagnetic hexagonal spin clusters rather than individual spins. In effect, ZnCr_2O_4 at low temperatures is not a system of strongly interacting spins, but a ‘protectorate’ of weakly interacting spin-loop directors. (The term ‘protectorate’ was introduced⁸ to describe stable states of matter in strongly correlated many-body systems. As antiferromagnetic hexagonal spin loops appear to be stable composite degrees of freedom for the pyrochlore lattice, we call the corresponding low-temperature state of the frustrated magnet a protectorate.)

Thermal and quantum fluctuations that violate collinearity within the hexagons should induce residual interactions between directors. Such interactions may account for the inelasticity of the scattering, the director correlations reflected in the greater sharpness of the experimental features in Figs 2 and 3, and the increase of κ with T , which indicates gradual disintegration of the directors.

What is the basis for the emergence of spin-loop directors as the effective degrees of freedom in this frustrated magnet? Fig. 4 shows the spins surrounding a hexagon in the pyrochlore lattice. Spin configurations that satisfy all interactions are characterized by the connected vectors of Fig. 4b. Although the spin configuration

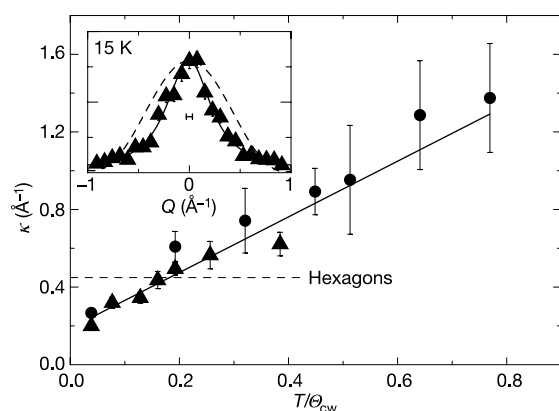


Figure 2 Temperature dependence of the inverse correlation length, $\kappa(T) = \xi(T)^{-1}$. (Temperature is given in units of the Curie–Weiss temperature, Θ_{CW} .) The data were derived from antiferromagnetic neutron scattering peaks by fitting to resolution-convoluted lorentzians. The triangles and circles are the lorentzian HWHMs along the $(h/4 \ 5/4)$ direction for $\hbar\omega = 1 \text{ meV}$, obtained with seven and eleven analyser blades, respectively. κ does not vanish as $T/|\Theta_{\text{CW}}| \rightarrow 0$, but extrapolates to a value that is close to the HWHM associated with the squared form factor for antiferromagnetic hexagon spin loops (dashed line). Inset, raw data for ZnCr_2O_4 at $T = 15 \text{ K}$. The bar shows the experimental resolution. The solid line is a resolution convoluted two-dimensional lorentzian; the dashed line is the squared hexagon spin-loop form factor convoluted with resolution.

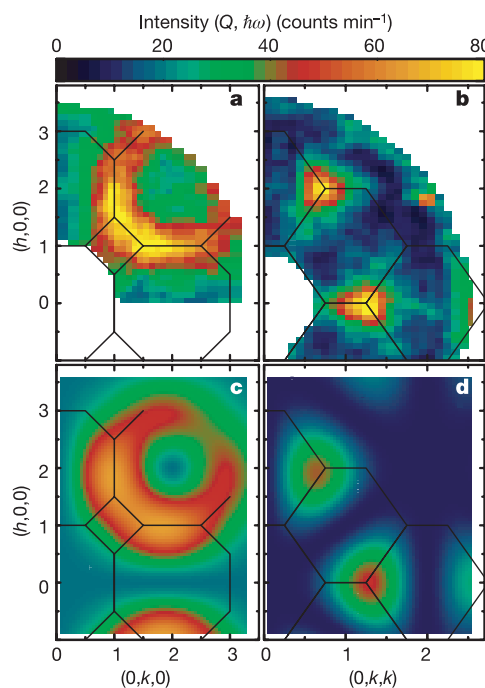


Figure 3 Wavevector dependence of the inelastic neutron scattering cross-section for ZnCr_2O_4 . **a, b**, Colour images of inelastic neutron scattering intensities from single crystals of ZnCr_2O_4 in the $(hk0)$ and (hkk) symmetry planes obtained at $T = 15 \text{ K}$ for $\hbar\omega = 1 \text{ meV}$. The data are a measure of the dynamic form factor for self-organized nanometre-scale spin clusters in the material. **c, d**, Colour images of the form factor squared calculated for antiferromagnetic hexagon spin loops averaged over the four hexagon orientations in the spinel lattice. The excellent agreement between model and data identifies the spin clusters as hexagonal spin loops.

remains severely under-constrained, no adjustment is possible without affecting spins on the outer perimeter. A general lowest-energy spin configuration on the pyrochlore lattice should therefore have wave-like soft modes that extend throughout the lattice. However, if the six hexagon spins are antiparallel with each other (Fig. 4c), then the staggered magnetization vector for a single hexagon, which for brevity we shall call the spin-loop director, is decoupled from the 12 outer spins, and hence its reorientation embodies a local zero energy mode for the pyrochlore lattice¹². It is possible to assign simultaneously all spins on the spinel lattice to hexagons, thus producing $N/6$ (where N is total number of spins) weakly interacting degrees of freedom (Fig. 1c). Accordingly, states that account for 1/6 of the entropy of the magnet are accessible through local fluctuations from configurations where all spins are bunched into directors. Indeed, the measured entropy of $0.15 R \ln 4$ (where R is the gas constant) just above a low-temperature spin-Peierls-like phase transition^{4,13} is close to the predicted entropy of $(1/6) R \ln 4$ for uncorrelated directors in a spin-3/2 magnet. In contrast, there are no local soft modes for a general spin configuration in the low-energy manifold. This distinction between a general state from the low-energy manifold and states from the director protectorate is probably the basis for the stability of the latter.

Our finding that fluctuations in ZnCr_2O_4 involve spin clusters and not individual spins provides a natural explanation for a range of properties of geometrically frustrated magnets. It explains why the temperature-dependent susceptibility of frustrated magnets is accurately described by exact diagonalization of judiciously chosen spin clusters^{14–16}. Moreover, the so-called ‘undecouplable’ muon spin resonance response¹⁷ is recognized as being a consequence of muons sensing slow, large-amplitude fluctuations of select spins in a spin director. A director protectorate also provides a natural explanation for the coexistence of low characteristic energy scales with rigid short-range order, as evidenced by specific-heat¹⁸ and quasi-elastic neutron data¹⁹.

The director protectorate hints at an organizing principle for frustrated systems: if macroscopic condensation is not possible, interacting degrees of freedom combine to form rigid composite entities or clusters with weak mutual interactions. Exploring the

generality and basis for such a principle should be an interesting focus for theoretical work and experiments on a wider class of systems. Composite degrees of freedom are common in strongly interacting many-body systems. Quarks form hadrons, hadrons form nuclei, nuclei plus electrons form atoms, and atoms form molecules, which in turn are the basis for complex biological functionality. Planets, stars, galaxies and galaxy clusters are examples of clustering on a grander length scale. However, to our knowledge, the emergence of a confined spin cluster degree of freedom has not previously been documented in a uniform gapless magnet. The discovery is important because magnets offer an opportunity not afforded by the above-mentioned systems to monitor emergent structure in complex interacting systems with microscopic probes such as neutron scattering and NMR. The collapse of a geometrically frustrated magnet into a director protectorate could, for example, be a useful template for exploring aspects of protein folding^{2,20}. □

Methods

Three crystals of ZnCr_2O_4 (total mass 200 mg) were co-mounted for the inelastic neutron scattering measurements. The measurements were performed using the cold neutron triple-axis spectrometer SPINS at the National Institute of Standards and Technology Center for Neutron Research. A vertically focusing pyrolytic graphite (002) monochromator, PG(002), extracted a monochromatic beam with energy $E_i = 6.1$ meV from a ^58Ni -coated cold neutron guide. Scattered neutrons were analysed with seven or eleven $2.1 \text{ cm} \times 15 \text{ cm}$ PG(002) analyser blades that reflected neutrons with $E_f = 5.1$ meV onto a ^3He proportional counter. Cooled Be filtered the scattered beam. Received 22 February; accepted 4 July 2002; doi:10.1038/nature00964.

1. Debenetti, P. G. & Stillinger, F. H. Supercooled liquids and the glass transition. *Nature* **410**, 259–267 (2001).
2. Wolynes, P. G. & Eaton, W. A. The physics of protein folding. *Phys. World* **12**, 39–44 (1999).
3. Bramwell, S. T. & Gingras, M. J. P. Spin ice state in frustrated magnetic pyrochlore materials. *Science* **294**, 1495–1501 (2001).
4. Ramirez, A. P. in *Handbook on Magnetic Materials* (ed. Busch, K. J. H.) Vol. **13**, 423–520 (Elsevier Science, Amsterdam, 2001).
5. Moessner, R. & Chalker, J. T. Properties of a classical spin liquid: the Heisenberg pyrochlore antiferromagnet. *Phys. Rev. Lett.* **80**, 2929–2932 (1998).
6. Canals, B. & Lacroix, C. Pyrochlore antiferromagnet: a three-dimensional quantum spin liquid. *Phys. Rev. Lett.* **80**, 2933–2936 (1998).
7. Stormer, H. L., Tsui, D. C. & Gossard, A. C. The fractional quantum Hall effect. *Rev. Mod. Phys.* **71**, S298–S305 (1999).
8. Laughlin, R. B. & Pines, D. The theory of everything. *Proc. Natl Acad. Sci. USA* **97**, 28–31 (2000).
9. Lovesey, S. W. *Theory of Thermal Neutron Scattering from Condensed Matter* (Clarendon, Oxford, 1984).
10. Birgeneau, R. J. et al. Instantaneous spin correlations in La_2CuO_4 . *Phys. Rev. B* **59**, 13788–13794 (1999).
11. Lee, S.-H. et al. Spin-glass and non-spin-glass features of a geometrically frustrated magnet. *Europhys. Lett.* **35**, 127–132 (1996).
12. Moessner, R. & Chalker, J. T. Low-temperature properties of classical, geometrically frustrated antiferromagnets. *Phys. Rev. B* **58**, 12049–12062 (1998).
13. Lee, S.-H., Broholm, C., Kim, T. H., Rattliff, W. & Cheong, S.-W. Local spin resonance and spin-Peierls-like phase transition in a geometrically frustrated antiferromagnet. *Phys. Rev. Lett.* **84**, 3718–3721 (2000).
14. Moessner, R. & Berlinsky, A. J. Magnetic susceptibility of diluted pyrochlore and $\text{SrCr}_{9-x}\text{Ga}_{3+x}\text{O}_{19}$. *Phys. Rev. Lett.* **83**, 3293–3296 (1999).
15. Garcia-Adeva, A. J. & Huber, D. L. Quantum tetrahedral mean-field theory of the pyrochlore lattice. *Can. J. Phys.* **79**, 1359–1364 (2001).
16. Mekata, M. & Yamada, Y. Magnetic-ordering process in $\text{SrCr}_2(\text{Ga-In})_2\text{O}_{19}$. *Can. J. Phys.* **79**, 1421–1426 (2001).
17. Uemura, Y. J. et al. Spin fluctuations in frustrated kagomé lattice system $\text{SrCr}_8\text{Ga}_4\text{O}_{19}$ studied by muon spin relaxation. *Phys. Rev. Lett.* **73**, 3306–3309 (1994).
18. Ramirez, A. P., Espinosa, G. P. & Cooper, A. S. Elementary excitations in a diluted antiferromagnetic kagomé lattice. *Phys. Rev. B* **45**, 2505–2508 (1992).
19. Broholm, C., Aeppli, G., Espinosa, G. P. & Cooper, A. S. Antiferromagnetic fluctuations and short range order in a kagomé lattice. *Phys. Rev. Lett.* **65**, 3173–3176 (1990).
20. Pande, V. S., Grosberg, A. Yu. & Tanaka, T. Heteropolymer freezing and design: Towards physical models of protein folding. *Rev. Mod. Phys.* **72**, 259–314 (2000).

Acknowledgements

We thank O. Tchernyshyov, R. Moessner, S. L. Sondhi, A. B. Harris, G. Aeppli, N. Read and D. Weitz for discussions, J. J. Rush, A. P. Ramirez and P. M. Gehring for critical reading of the manuscript, and Z. Huang for assistance in making figures. This work was partially supported by the NSF and the BSF.

Competing interests statement

The authors declare that they have no competing financial interests.

Correspondence and requests for materials should be addressed to S.H.L. (e-mail: shl@nist.gov).

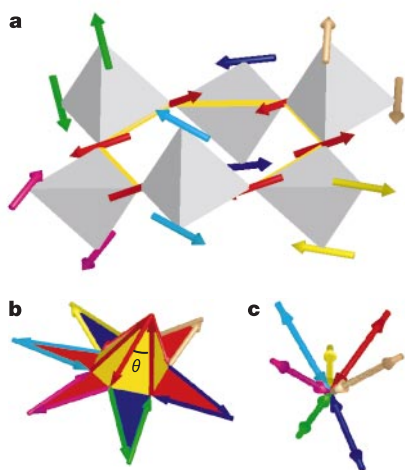


Figure 4 Possible spin fluctuations in the classical ground-state manifold. **a**, Spin cluster surrounding a hexagon (shown in yellow) in the pyrochlore lattice of Fig. 1c. **b**, Generalized pattern of classical spin vectors on six neighbouring tetrahedra satisfying the condition that there be no net spin on any tetrahedron. **c**, Pattern of spin vectors satisfying the condition that $\theta = 0$ for all tetrahedra. For such spin configurations, each tetrahedron has two pairs of antiparallel spins, and each hexagon has six collinear and antiferromagnetic spins as indicated by six red arrows in **a**. The energy of the spin cluster is independent of the orientation of the spin-loop directors.